ICES CM 2009/T:08

Modelling the sources of mortality for larval haddock on Georges Bank and their effects on behavior

Colleen M. Petrik[1], Cabell S. Davis[1], Rubao Ji[1], R. Gregory Lough[2], Trond Kristiansen[3]

[1]Biology Department, Woods Hole Oceanographic Institution, Woods Hole, MA 02543, USA
[2]Institute of Marine Research, P.O. Box 1870 Nordnes, 5817 Bergen, Norway
[3]Northeast Fisheries Science Center, NMFS, NOAA, Woods Hole, MA 02543, USA

e-mail contact: cpetrik@whoi.edu

ABSTRACT

Fish larvae have the ability to change their vertical position in the water column and thusly cannot be treated as passive particles in coupled biological-physical individual-based models (IBMs). The vertical variability of light, turbulence, temperature, prey, predators, and horizontal currents in the ocean affects the survival of larval fish through effects on feeding, growth, advection, and predation mortality. A dynamic model of the vertical position of larval fish in response to individual state and environmental conditions is needed for use in three-dimensional IBMs. A 1-dimensional model was constructed of an idealized water column representative of spring conditions on the southern flank of Georges Bank. The water column was used to test six behavioral rules of individuals parameterized as larval haddock (*Melanogrammus aeglefinus*) under different conditions of prey and turbulence stratification. Our objectives were to determine how behaviors based on different state and environmental variables affect depth distribution and mortality, and which behaviors produce a vertical distribution most similar to observations. Individuals applying behaviors associated with feeding had distributions comparable to observations and the highest survival. The use of behaviors derived from a trade-off between gut fullness and visual predation led to distributions unlike observations and high starvation mortality of the largest larval size class. Results suggest that larvae should make their vertical behavior decisions based on the risk of starvation rather than predation. A realistic model of larval haddock vertical position could be developed using only behaviors related to its prey distribution and foraging success.

INTRODUCTION

Three-dimensional (3D) coupled biological-physical individual-based models (IBMs) are used to study the early life stages of fish. These Lagrangian models have been used to study the timing and placement of spawning (Brickman & Frank 2000, Hinckley et al. 2001, Mullon et al. 2002, Lough et al. 2006), growth during the larval period (Letcher et al. 1996, Werner et al. 1996, Lough et al. 2005, Kühn et al. 2008, Kristiansen et al. *in*

press), contributions of starvation, predation, and advective mortality (Werner et al. 1996, Brickman et al. 2001), arrival at the juvenile habitat (Hinckley et al. 2001, Mullon et al. 2002, Lough et al. 2006), and characteristics of larvae that survive to the juvenile transition (Cowan et al. 1997, Mullon et al. 2002). Numerous studies have verified that larvae are not passive particles, but can moderate their vertical position in the water column (Leis 2007). An accurate representation of larval vertical position is important in these models because it affects survival in a number of ways. Differences in light, turbulence, and prey concentration with depth result in different amounts of prey encountered and ingested, which affects starvation. Temperature regulates metabolic processes like growth and respiration such that vertical gradients could also influence starvation. Horizontal currents carry larvae toward or away from suitable habitat, and their vertical shear could result in advective loss. Finally, variations in predator abundance and consumption rate with depth cause direct losses of larvae. The losses of larvae through starvation, advection, and predation result in new vertical distributions.

Previous IBMs use either passive particles (e.g. Werner et al. 1996, Mullon et al. 2002) or assign depths to given stages/ages based on observations (e.g. Lough et al. 2005, Kühn et al. 2008). Though assigning depths is a step above passivity, it does not allow larvae to alter their depth with changes to their environment. Observations of larval haddock (*Melanogrammus aeglefinus*) and cod (*Gadus morhua*) on Georges Bank show that vertical distributions are correlated with the strength of stratification such that the abundance maximum becomes associated with the pycnocline as stratification increases (Lough 1984, Buckley & Lough 1987, Lough & Potter 1993). Water column stratification changes on Georges Bank over the course of the larval duration from seasonal heating, wind events, and location (well-mixed on the crest, stratified on the flanks). Thus, a model of larval haddock on Georges Bank should be able to account for these differences in depth position.

To build a 3D model of larval haddock on Georges Bank, first a model of the vertical position of individuals in response to environmental variables is needed. Larvae sense and respond behaviorally to aspects of their environment (e.g., light, gravity, temperature), which results in a nonrandom depth distribution. In the simplest case, larvae are unlikely to sense prey gradients because their perception area is too small to encounter more than one prey at a time and such an ability would require a memory. For this same reason larvae probably cannot sense predation risk gradients, but may be able to sense the presence or absence of predators though sight or chemical cues. By contrast, larvae should have a sense of their state of hunger or gut fullness that could help them make behavioral decisions.

We constructed a 1D water column similar to the Georges Bank southern flank in the spring with varying conditions of stratification. Different vertical behavior models using various state and environmental variables were tested to determine (1) how each behavior affects depth distribution, (2) how each behavior affects mortality, and (3) which behavior results in a vertical distribution most similar to observations.

MODELS AND METHODS

Initialization

Three different size classes of larvae were simulated: 5 mm, 6-8 mm, and 9-13 mm. The model was run for 10 days with 1000 individuals of each size class. Individuals were initialized at a random depth with 10% gut fullness.

Environment

The environment is representative of the southern flank of Georges Bank in May. Some maximum and mean values of environmental conditions were taken from a study tracking a cohort of larval fish in May of 1993 and 1994 (Lough et al. 2005). The depth of the water column is 70 m, with the base of the mixed layer (*dmix*) at 30 m.

Light

Light decays with depth following

$$E(z) = E_0 \exp(-0.18z).$$

To test the effects of light with depth and daily changes in light, two different light conditions were used: always noon and full light cycle. When it was always noon

$$E_0 = E_{\max} = 500 \ \mu\text{mol m}^{-2}\ \text{s}^{-1}.$$

The full light cycle was modeled as

$$E_0 = E_{\max} \sin\left(\frac{2\pi \cdot hr}{24}\right)$$

with $E_0 = 0$ for negative values.

Temperature

Temperature was held constant at 7.8°C, the average of a stratified 70 m water column with maximum of 9°C and minimum of 7°C and a thermocline at 30 m.

Turbulence

Under uniform conditions the dissipation rate (W kg^{-1}), ε, was 5.0e-7, the average of the 1993 and 1994 observations. When stratified the dissipation rate took the form

$$\varepsilon(z) = \max * \left(1 - \exp\left(\frac{(z - dmix)^2}{20 * dmix}\right)\right) + \min$$

with max=1e-4 and min=1e-8, the maximum and minimum measured in 1994. Both conditions are depicted in Fig. 1a.

Prey

For simplification, only one type of prey was available for consumption. The copepod *Pseudocalanus* spp. was selected because it is the majority of the prey biomass consumed by larval haddock (Kane 1984, Lough et al. 2005, Heath & Lough 2007) and its biomass is highly correlated to larval haddock growth rate (Buckley & Durbin 2006). The developmental stage of *Pseudocalanus* spp. was set as the largest stage with positive preference as determined by Petrik et al. (*in press*) for each size class (Table 1). Stratified prey were represented as

$$prey(z) = \max * \left(\exp\left(\frac{(z - dmix)^2}{2 * dmix}\right)\right)$$

with the maximum set as the mean of the 1993 and 1994 observations of maximum number per liter of that prey stage (Table 1). Under uniform prey conditions, the density

was equal to the depth integrated mean of the stratified conditions (Table 1). Fig. 1b illustrates the relative prey abundance depth profiles of both uniform and stratified conditions.

Table 1. Developmental stage of *Pseudocalanus* spp., its maximum and mean values (# L^{-1}) for each size class of haddock. N: nauplii, C: copepodite.

Size class	Prey stage	Prey max	Prey mean
5 mm	NIV	2.50	0.4903
6-8 mm	CII	0.30	0.0588
9-13 mm	CIVf	0.25	0.0490

Foraging submodel

The foraging submodel was based on the larval fish feeding models of Caparroy et al. (2000), Fiksen & MacKenzie (2002) and Kristiansen et al. (2007), and was parameterized for larval haddock and *Pseudocalanus* spp. by Petrik et al. (*in press*). The model mechanistically simulated the foraging cycle of encounter, pursuit, capture, and ingestion of copepod prey. In this model ingestion was the product of encounter rate and the probability of successful capture. Encounter rate was a function of the larval fish pause-travel swimming characteristics (pause duration and frequency), the larval perception distance dependent on light and larval size, prey density, prey swimming speed, and turbulent velocity. The probability of successful capture is a function of species-specific prey escape behaviors: the deformation rate threshold, escape jump speed, and escape jump angle. For computational speed, the probability was parameterized to be a function of prey species and stage length using the results of Petrik et al. (*in press*) instead of simulating the whole process.

Bioenergetics submodel

The bioenergetics submodel was the same as that used in Petrik et al. (*in press*) for larval haddock, which was based on Kristiansen et al. (2007) for larval cod. The amount of biomass ingested in the foraging submodel was tracked and the energy derived from it was apportioned to metabolism and growth, both of which were temperature and larval size dependent. Metabolism was increased a constant amount during light hours to account for the activity of feeding fish. Additionally, swimming vertically cost energy proportional to the distance traveled.

Vertical behavior models

Six different vertical behavior models were tested. All use the same maximum swimming speed as a function of body length (BL) derived by Peck et al. (2006) from the closely related species Atlantic cod,

$$w_{\max} = 0.261 * BL^{1.552 * BL^{-0.08}} - 5.289/BL.$$

Case A

Swimming speed decreases as encounter rate increases, following the idea that handling time, which increases with encounter rate, decreases the amount of time swimming. Direction up (defined as positive) or down (defined as negative) is random.

$$w = \pm w_{\max}\left(1 - \left(\frac{enc}{enc_{\max}}\right)\right)$$

The maximum encounter rate, enc_{max}, was determined for each size class under water column conditions of only stratified prey, and both stratified prey and turbulence. If turbulence was uniform in the simulations (regardless of prey distribution) enc_{max} was set as that with stratified prey (Table 2). If turbulence was stratified, enc_{max} was set as that under stratified prey and turbulence (Table 2).

Table 2. Values of enc_{max} for different size classes and turbulence conditions.

	5 mm	6-8 mm	9-13 mm
uniform turbulence	5.09E+03	5.18E+03	6.77E+04
stratified turbulence	6.25E+03	5.78E+03	7.57E+04

Case B

Swimming speed decreases as prey concentration increases, following the theory that handling time, which increases with prey concentration, decreases the amount of time swimming. Direction is random.

$$w = \pm w_{\max}\left(1 - \left(\frac{prey}{prey_{\max}}\right)\right)$$

In all simulations the maximum prey, $prey_{max}$, is the maximum of the stratified conditions depending on size class (Table 1).

Case C

Since larvae may not be able to detect prey density or encounter rate, state of hunger was used to make the vertical behavior decision. Swimming speed decreases as gut fullness, *gut*, increases, with random direction,

$$w = \pm w_{\max}(1 - gut).$$

The concepts behind this behavior are that a full gut denotes recently handled prey that decreases swimming and/or that hungry larvae may swim faster to find prey patches.

Case D

Swimming speed increases as gut fullness increases, possibly because hungry larvae have less energy for swimming. Direction is random.

$$w = \pm w_{\max} \cdot gut$$

Case E

Vertical position can be viewed as habitat selection chosen to maximize fitness as defined by some formulation of maximizing feeding/growth and minimizing predation mortality (Werner et al. 1983, Gilliam & Fraser 1987, Aksnes & Giske 1990, Kristiansen et al. 2009). Since we are assuming that larvae cannot detect gradients in predation risk but can detect light, light represents the risk of predation by visual feeders. Swimming speed and direction are determined by a trade-off, *T*, between gut fullness and light

$$T = \alpha(1 - gut) - \beta\left(\sqrt{\frac{light}{1 + light}}\right) \qquad \text{with } \beta = 1 - \alpha$$

$$\text{if } T\begin{cases} > 0 \\ < 0 \\ = 0 \end{cases} \text{ then } w = \begin{cases} w_{\max} \\ -w_{\max} \\ 0 \end{cases}.$$

The form of the light component of the model was chosen because that is relationship light has with encounter rate for visual predators. When a larva is hungry and light is low it should swim up to where there is more light to see prey, and when it is full and light is strong it should swim down to avoid visual predators. How much weight is placed on the importance of hunger and predation depends on α and β.

Case F

Swimming speed and direction are determined by the trade-off, *T*, between gut fullness and light. When hunger is stronger than avoiding light, individuals decrease their swimming speed as prey density increases, with random direction.

$$T = \alpha(1 - gut) - \beta\left(\sqrt{\frac{light}{1 + light}}\right) \qquad \text{with } \beta = 1 - \alpha$$

$$\text{if } T\begin{cases} > 0 \\ < 0 \\ = 0 \end{cases} \text{ then } w = \begin{cases} \pm w_{\max} \cdot (1 - (prey / prey_{\max})) \\ -w_{\max} \\ 0 \end{cases}.$$

Simulations

Four different environmental conditions were run for each size class: (1) uniform prey and turbulence, (2) stratified prey and uniform turbulence, (3) stratified prey and turbulence, and (4) uniform prey and stratified turbulence. Cases 4 and 5 were run with α values of 0.25, 0.50, 0.75, 0.99, and random.

RESULTS

The following results were simulated under noon light conditions where the surface light was always equal to the maximum. This situation represents the best possible scenario for larval feeding, as encounter rate is proportional to light.

Depth distributions

Case A

Individuals are distributed throughout the water column when prey is uniform, regardless of turbulence (Fig. 2a). When prey is stratified and turbulence is uniform, individuals aggregate at the prey maximum at the base of the mixed layer (Fig. 2b). When prey and turbulence are stratified there is lower abundance at the base of the mixed layer and the maximum is shifted to just above it (Fig. 2c).

Case B

The distribution of larvae mimics their prey regardless of turbulence (Fig. 3a,b). Stratification of larvae is stronger than in Case A.

Case C

The depth of maximum abundance is between 50 and 60 m when prey and turbulence are uniform (Fig. 4a). When prey is stratified, most individuals are between 10 and 45 m, with a peak at 45 m (Fig. 4b). When prey is uniform but turbulence is stratified the 5 mm and 9-13 mm larvae are well-mixed, but the 6-8 mm larvae aggregate at 60 m (Fig. 4c).

Case D

When prey and turbulence are uniform, abundance peaks between 60 and 70 m (Fig. 5a). There is a bimodal distribution with maxima at the surface and 50 m when prey is stratified (Fig. 5b). Similar to Case C, when prey is uniform but turbulence is stratified the 5 mm and 9-13 mm larvae are well-mixed, and the 6-8 mm larvae aggregate between 60 and 70 m (Fig. 5c).

Case E

Most size classes have maximum abundance at 45 m under most environmental conditions (e.g. Fig. 6a) with the following exceptions. When prey and turbulence are uniform, 5 mm and 6-8 mm larvae aggregate at 60 m and 9-13 mm at 70 m for all values of α except for 0.99 (e.g. Fig. 6b). When turbulence is stratified and α=0.99, the 6-8 mm larvae shift from a maximum at 50 m to one at 40m over the 10 days, while the 9-13 mm larvae have peak abundance near 40 m (Fig. 6c). For all other values of α with stratified turbulence, all size classes are between 65 and 70 m depth (e.g. Fig. 6d).

Case F

When prey is stratified all individuals aggregate between 50 and 70 m (e.g. Fig. 7a). When prey is uniform and α is anything but 0.99, larvae are in the bottom 60-70 m (e.g. Fig. 7b). Individuals are higher when prey is uniform and α=0.99, with all sizes starting concentrated at 50 m then spreading out between 50 and 60 m for 5 mm, and between 50 and 70 m for 6-8 mm and 9-13 mm (Fig. 7c).

Survival

There was 100% survival of 5 mm larvae in every behavioral case and environmental scenario. There was 100% survival of 6-8 mm in all environmental conditions with Cases A, E, and F. Individuals using Case B had 99.2-100% survival, with the lowest under stratified prey and turbulence. Individuals using Case C had 99.4-100% survival, with the lowest under stratified prey and uniform turbulence. Individuals using Case D had 99.6-100% survival, with the lowest under uniform prey and turbulence. The 9-13 mm size class showed the greatest variation in survival (Table 3). Larvae with Case A behavior had very poor survival of 0% under uniform prey conditions and 0.1% with stratified prey. Survival using Case B was much higher with stratified prey (65.9-66.5%) than uniform prey (2.4-2.5%). There was high survival of individuals using Case C. It was 100% with uniform prey and 96.4-97.9% when prey was stratified. Case D larvae had the highest survival (50.5-51%) when prey was stratified, lower survival of 10.5% when prey and turbulence were uniform, and 0% survival when prey was uniform and turbulence was stratified. No 9-13 mm individuals survived using Case E behavior. Case F only had survivors when α=0.99 or random. When α=0.99 and random, survival was 2.2% and 19.2% respectively with uniform prey and turbulence, and 3.1% and 2.6% with uniform prey and stratified turbulence. Only individuals with random α survived when prey was stratified. Under stratified prey survival was 0.3% when turbulence was uniform and 0.5% when turbulence was stratified. The range of α values of the survivors were 0.0823-0.9953 with uniform prey and turbulence, 0.9953-0.9987 with stratified prey and uniform turbulence, 0.9938-0.9983 with stratified prey and turbulence, and 0.9031-0.9953 with uniform prey and stratified turbulence.

Table 3. Percent survival of 9-13 mm larvae under different environmental conditions and behavior strategies.

	Prey	uniform	stratified	stratified	uniform
	Turbulence	uniform	uniform	stratified	stratified
Case	α				
A	N/A	0	0.1	0.1	0
B	N/A	2.4	65.9	66.5	3.5
C	N/A	100	96.4	97.9	100
D	N/A	10.5	51.0	50.5	0
E	0.25	0	0	0	0
E	0.50	0	0	0	0
E	0.75	0	0	0	0
E	0.99	0	0	0	0
E	random	0	0	0	0
F	0.25	0	0	0	0
F	0.50	0	0	0	0
F	0.75	0	0	0	0
F	0.99	2.2	0	0	3.1
F	random	19.2	0.3	0.5	2.6

DISCUSSION

Changing one aspect of the environment at a time allowed for easy interpretation of the depth distribution and survival results. When individuals used behavioral Cases A and B the depth distributions generally followed their prey. Case A differed because turbulence affects encounter rate. The low turbulence at the base of the mixed layer reduced encounter rate and shifted the maximum abundance to just above this depth. It was shifted above rather than below the base of the mixed layer because of the positive effects of light. Stratification of larvae was stronger using Case B because a more well-defined $prey_{max}$ led to swimming speeds closer to zero, allowing more individuals to maintain position in the prey maximum. The enc_{max} value was the largest encounter rate that any individual could reach in a stratified prey simulation, which was ultimately the encounter rate of the largest individual possible in a simulation. For example, in simulations of the 9-13 mm size class, the enc_{max} was set by 13 mm larvae, thus 9-12 mm larvae would never encounter that many prey and their velocity would never reach zero. This was an unrealistic scenario for the behavioral model and this scenario would not be possible in a dynamic 3D model simulation. Both of these behaviors produced depth distributions similar to observations of larval haddock where maximum densities coincided with the depth of highest prey biomass (Lough 1984, Buckley & Lough 1987, Lough & Potter 1993). Like observations of larvae following storm-induced mixing events (Lough 1984, Lough & Potter 1993), modeled larvae using Case B that began uniformly (randomly) spaced in the water column were able to stratify in a few days if their prey were already stratified.

Cases C and D are inverses of each other, thus resulting in opposite depth distributions. When prey was stratified, guts were 100% between 10 and 45 m. Thus when larvae applied Case C they were between these depths, and when they used Case D they were above and below these depths. The maximum at 45 m seen in Case C was caused by the greater number of larvae below 45 m swimming up, than the number of larvae above 10 m swimming down. Aggregation did not intensify in the middle because these larvae had full guts and zero velocity. When prey and turbulence were uniform, all guts were full down to a depth around 60 m where light became limiting. When Case C was employed aggregation occurred just above this depth as the larvae below it swam out of it. Conversely, when Case D was used there was a maximum below 60 m that individuals swam into. When prey was uniform but turbulence was stratified the 5 mm and 9-13 mm larvae were well-mixed, but the 6-8 mm larvae aggregated near 60 m. The different distribution of 6-8 mm larvae was related to their gut fullness in comparison to the other size larvae. A combination of prey density, prey biomass, and metabolism specific to the 6-8 mm larvae resulted in guts that were much more empty than either the 5 mm or 9-13 mm larvae. Thus their swimming speeds were much closer to zero, resulting in a maximum at the depth where gut fullness changed from 100% to 0%. It is more realistic for the swimming speed of larval haddock to be inversely proportional to gut fullness since the Case C distribution of larvae was more like observations than Case D.

Larvae using both Cases E and F were very deep in the water column. The very strong noon light conditions often outweighed hunger, such that larvae were located at the depth where light became limiting.

Under stratified prey conditions, the number of surviving 9-13 mm larvae increased as Case E < A < F < D < B <C. Case C individuals had the highest survival because larvae swam out of the area causing empty guts, thus avoiding starvation. There were more survivors when Case B was used compared to Case D because more larvae were closer to the prey maximum. Though both Cases A and B had similar depth distributions, Case B had more survivors because fewer larvae using Case A were able to move into and stay in the prey maximum over the course of 10 days, leading to high starvation of the 9-13 mm size class.

All 9-13 mm individuals using Case E starved because their behavior forced them to a depth where it was difficult to see prey. Certain 9-13 mm larvae were able to survive using the Case F behavior depending on their α value and the environment. When prey and turbulence were uniform only light differed with depth, so a wide range of α values were able to survive. When prey was stratified only high α values ≥ 0.99 were able to survive because a lot of weight needed to be placed on gut fullness to move individuals towards the prey maximum.

From these simulation experiments it appears that larval haddock should be more concerned with starvation mortality than predation. The larvae with higher survival rates were those that made behavioral decisions based on prey concentration and gut fullness alone. Thus it is better to be where the prey are as well as higher in the water column where there is more light to see. The risk of starvation emphasizes the importance of

having the right prey available. In these simulations the most preferred prey of larval haddock was used, but starvation losses could be greater if harder to catch species like *Centropages typicus* or *Calanus finmarchicus* (Petrik et al. *in press*) were the available prey. Starvation occurred when larvae used the two trade-off behaviors presented here that avoided visual predation. There are other predation avoiding strategies that may not result in starvation for larval haddock (Kristiansen et al. 2009). Furthermore, Lapolla and Buckley (2005) found that larvae that survived to the fall were spawned ahead of the peak, such that they were bigger in the late spring when predation is higher. Their findings imply that larvae may avoid predators in time rather than space.

The success of the prey density and gut fullness behaviors, and the failure of the trade-off behaviors suggest that larval haddock vertical behavior can probably be modeled with respect to some aspect of feeding alone. This is fortuitous because data on larval predator distributions and consumption rates on Georges Bank are lacking. Future work involves using the full light cycle, imposing predation losses, and use of the vertical behavior in a 3D model.

REFERENCES

Aksnes, D.L., and Giske, J. 1990. Habitat profitability in pelagic environments. Marine Ecology Progress Series, 64: 209-215.

Brickman, D., and Frank, K.T. 2000. Modelling the dispersal and mortality of Browns Bank egg and larval haddock (*Melanogrammus aeglefinus*). Canadian Journal of Fisheries and Aquatic Sciences 57: 2519-2535.

Brickman, D., Shackell, N.L., and Frank, K.T. 2001. Modelling the retention and survival of Browns Bank haddock larvae using an early life stage model. Fisheries Oceanography 10: 284-296.

Buckley, L.J., and Durbin, E.G. 2006. Seasonal and inter-annual trends in the zooplankton prey and growth rate of Atlantic cod (*Gadus morhua*) and haddock (*Melanogrammus aeglefinus*) larvae on Georges Bank. Deep-Sea Res II, 53: 2758-2770.

Buckley, L.J., and Lough, R.G. 1987. Recent growth, biochemical composition, and prey field of larval haddock (*Melanogrammus aeglefinus*) and Atlantic cod (*Gadus morhua*) on Georges Bank. Canadian Journal of Fisheries and Aquatic Sciences, 44: 14-25.

Caparroy, P., Thygesen, U.H., and Visser, A.W. 2000. Modelling the attack success of planktonic predators: patterns and mechanisms of prey selectivity. Journal of Plankton Research, 22: 1871-1900.

Cowan, J.H., Jr., Rose, K.A., and Houde, E.D. 1997. Size-based foraging success and vulnerability to predation: selection of survivors in individual-based models of larval fish populations. *In*: Early life history and recruitment in fish populations, pp. 357-386. Ed. by R.C. Chambers and E.A. Trippel. Chapman & Hall, London.

Fiksen, Ø., and MacKenzie, B.R. 2002. Process-based models of feeding and prey selection in larval fish. Marine Ecology Progress Series, 243: 151-164.

Heath, M.R., and Lough, R.G. 2007. A synthesis of large-scale patterns in the planktonic prey of larval and juvenile cod (*Gadus morhua*). Fisheries Oceanography, 16: 169-185.

Hinckley, S., Hermann, A.J., Mier, K.L., and Megrey, B.A. 2001. Importance of spawning location and timing to nursery areas: simulation study of Gulf of Alaska walleye pollock. ICES Journal of Marine Science, 58: 1042-1052.

Gilliam, J.F., and Fraser, D.F. 1987. Habitat selection under predation hazard: test of a model with foraging minnows. Ecology, 68: 1856-1862.

Kane, J. 1984. The feeding habits of co-occurring cod and haddock larvae from Georges Bank. Marine Ecology Progress Series, 16: 9-20.

Kristiansen, T., Fiksen, Ø., and Folkvord, A. 2007. Modelling feeding, growth, and habitat selection in larval Atlantic cod (*Gadus morhua*): observations and model predictions in a macrocosm environment. Canadian Journal of Fisheries and Aquatic Science, 64: 136-151

Kristiansen, T., Jørgensen, C., Lough, R.G., Vikebø, F., and Fiksen, Ø. 2009. Modeling rule-based behavior: habitat selection and the growth-survival trade-off in larval cod. Behavioral Ecology, 20: 490-500

Kristiansen, T., Vikebø, F., Sundby, S., Huse, G., and Fiksen, Ø. (*in press*). Modeling growth of larval cod (Gadus morhua) in large-scale seasonal and latitudinal environmental gradients. Deep-Sea Research II, doi:10.1016/j.dsr2.2008.11.011

Kühn, W., Peck, M.A., Hinrichsen, H.-H., Daewel, U., Moll, A., Pohlmann, T., Stegert, C., and Tamm, S. 2008. Defining habitats suitable for larval fish in the German Bight (southern North Sea): an IBM approach using spatially- and temporally-resolved size-structured prey fields. Journal of Marine Systems, 74: 329-342.

Lapolla, A., and Buckley, L.J. 2006. Hatch date distributions of young-of-year haddock *Melanogrammus aeglefinus* in the Gulf of Maine/Georges Bank region: implications for recruitment. Marine Ecology Progress Series, 290: 239-249.

Leis, J.M. 2007. Behaviour as input for modeling dispersal of fish larvae: behaviour, biogeography, hydrodynamics, ontogeny, physiology and phylogeny meet hydrography. Marine Ecology Progress Series, 347: 185-193.

Letcher, B.H., Rice, J.A., Crowder, L.B., and Rose, K.A. 1996. Variability in survival of larval fish: disentangling components with a generalized individual-based model. Canadian Journal of Fisheries and Aquatic Science, 53: 787-801.

Lough, R.G. 1984. Larval fish trophodynamic studies on Georges Bank: sampling strategy and initial results. *In* The propagation of cod *Gadus morhua*, pp. 395-434. Ed. by E. Dahl, D.S. Danielssen, E. Moskness, and P. Solemdal. Flødevigen rapportser I.

Lough, R.G., and Potter, D.C. 1993. Vertical distribution patterns and diel migrations of larval and juvenile haddock *Melanogrammus aeglefinus* and Atlantic cod *Gadus morhua* on Georges Bank. Fishery Bulletin, 91: 281-303.

Lough, R.G., Buckley L.J., Werner, F.E., Quinlan, J.A., and Pehrson Edwards, K. 2005. A general biophysical model of larval cod (*Gadus morhua*) growth applied to populations on Georges Bank. Fisheries Oceanography, 14: 241-262.

Lough, R.G., Hannah, C.G., Berrien, P., Brickman, D., Loder, J.W., and Quinlan, J.A. 2006. Spawning pattern variability and its effect on retention, larval growth and recruitment in Georges Bank cod and haddock. Marine Ecology Progress Series, 310: 193-212.

Mullon, C., Cury, P., and Penven, P. 2002. Evolutionary individual-based model for the

recruitment of anchovy (*Engraulis capensis*) in the southern Benguela. Canadian Journal of Fisheries and Aquatic Science, 59: 910-922.

Peck, M.A., Buckley, L.J., and Bengston, D.A. 2006. Effects of temperature and body size on the swimming speed of larval and juvenile cod (*Gadus morhua*): implications for individual-based modeling. Environmental Biology of Fishes, 75: 419-429.

Petrik, C.M., Kristiansen, T., Lough, R.G., and Davis, C.S. (*in press*) Prey selection of larval haddock and cod on copepods with species-specific behavior: a model-based analysis. Marine Ecology Progress Series.

Werner, E.E., Gilliam, J.F., Hall, G.D., and Mittelbach, G.G. 1983. An experimental test of the effects of predation risk on habitat use in fish. Ecology, 64:1540-1548.

Werner, F.E., Perry, R.I., Lough, R.G., Naimie, C.E. 1996. Trophodynamic and advective influences on Georges Bank larval cod and haddock. Deep-Sea Res II, 43: 1793-1822.

FIGURE LEGENDS

Fig. 1. Depth profile of uniform and stratified (a) turbulent dissipation rate ($\log_{10}(\varepsilon)$) in W kg^{-1} and (b) relative prey density in # L^{-1}. Each size class of larvae used a different prey density maximum, but the relationship between uniform and stratified concentrations were the same.

Fig. 2. Depth distribution of 1000 larvae using behavioral Case A over 10 days with (a) uniform prey and uniform or stratified turbulence, (b) stratified prey and uniform turbulence, and (c) stratified prey and turbulence.

Fig. 3. Depth distribution of 1000 larvae using behavioral Case B over 10 days with (a) uniform prey and uniform or stratified turbulence, (b) stratified prey and uniform or stratified turbulence.

Fig. 4. Depth distribution of 1000 larvae using behavioral Case C over 10 days with (a) uniform prey and uniform or stratified turbulence, (b) stratified prey and uniform or stratified turbulence, and (c) uniform prey and stratified turbulence.

Fig. 5. Depth distribution of 1000 larvae using behavioral Case D over 10 days with (a) uniform prey and uniform or stratified turbulence, (b) stratified prey and uniform or stratified turbulence, and (c) uniform prey and stratified turbulence.

Fig. 6. Depth distribution of 1000 larvae using behavioral Case E over 10 days with (a) stratified prey and uniform turbulence with α=random, (b) uniform prey and turbulence with α=random, (c) stratified prey and turbulence with α=0.99, (d) uniform prey and stratified turbulence with α=0.99, and (e) uniform prey and stratified turbulence with α=random.

Fig. 7. Depth distribution of 1000 larvae using behavioral Case F over 10 days with (a) stratified prey and turbulence with α=random, (b) uniform prey and turbulence with α=random, and (c) uniform prey and turbulence with α=0.99.

FIGURES

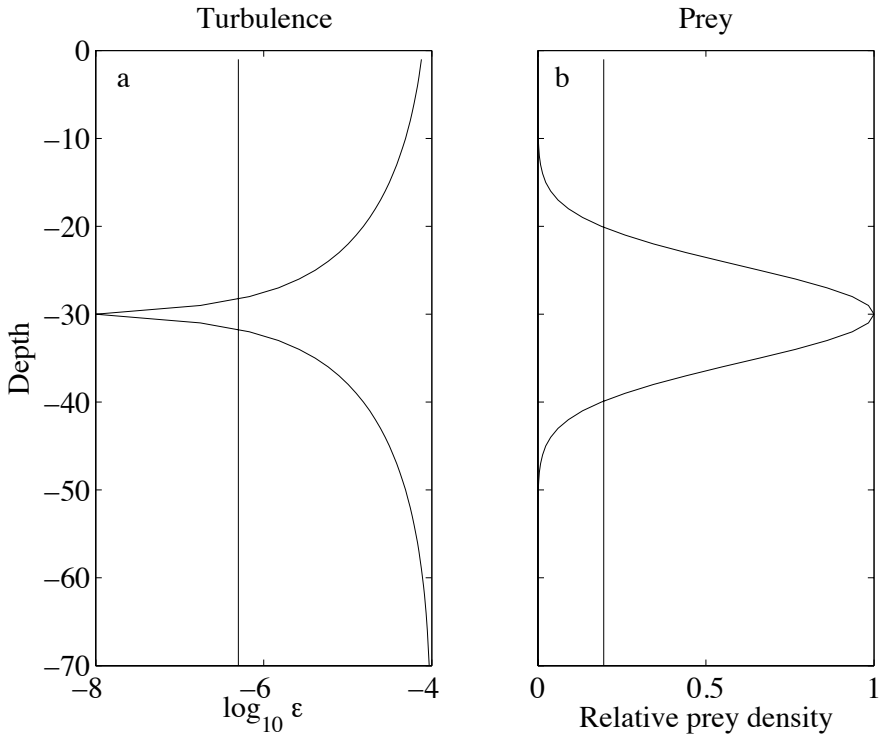

Fig. 1

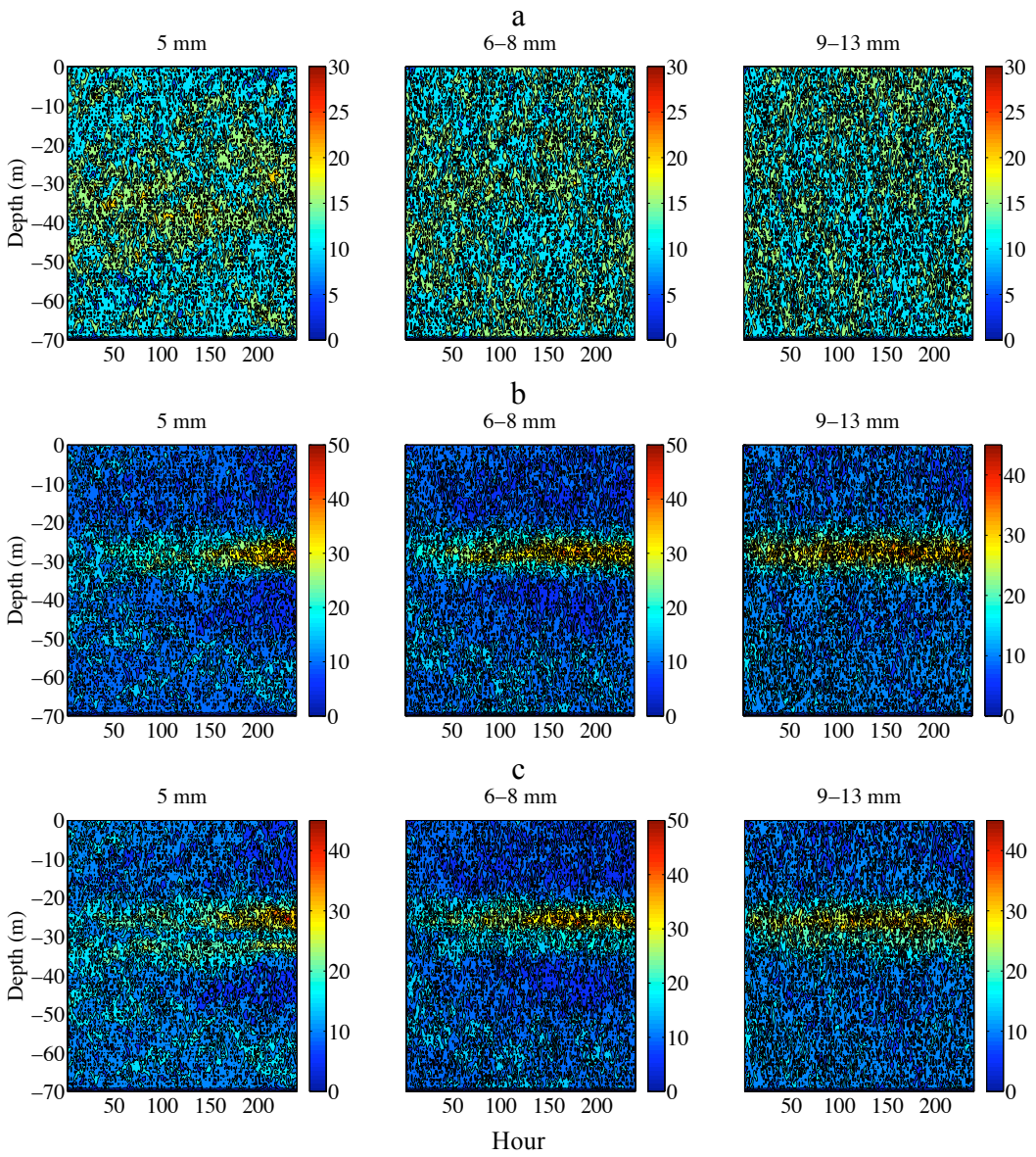

Fig. 2

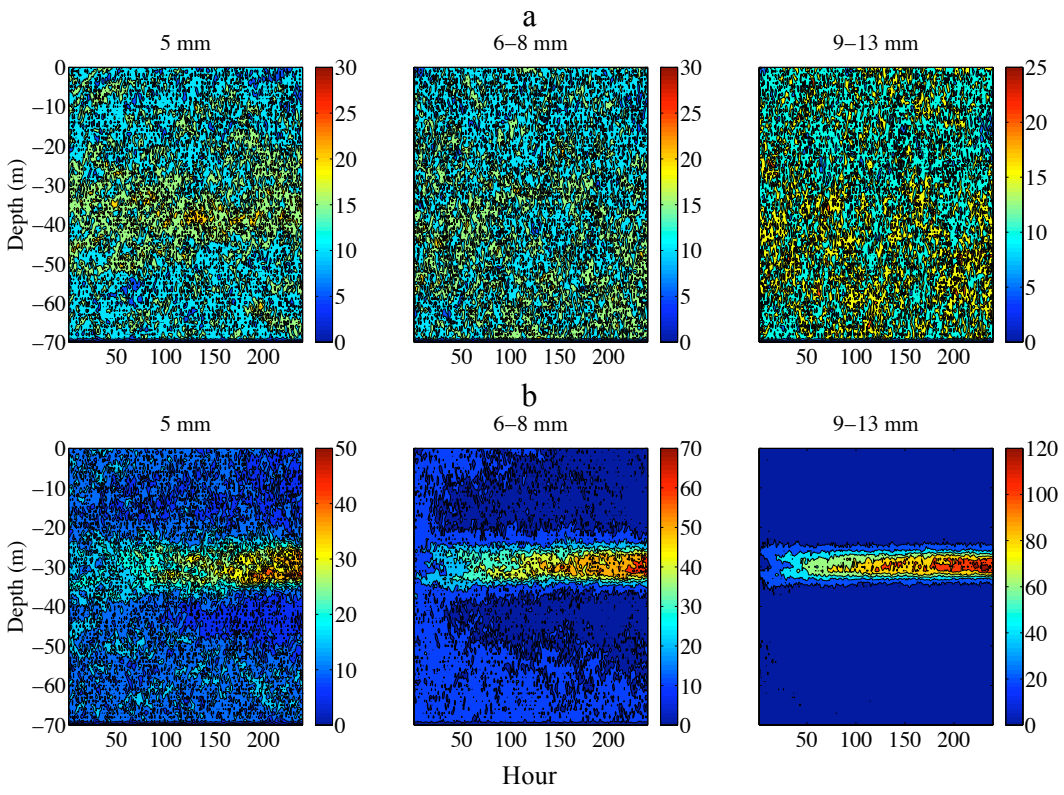
a
5 mm
6–8 mm
9–13 mm
Depth (m)
0
−10
−20
−30
−40
−50
−60
−70
50 100 150 200
30 25 20 15 10 5 0
25 20 15 10 5 0
b
5 mm
6–8 mm
9–13 mm
50 40 30 20 10 0
70 60 50 40 30 20 10 0
120 100 80 60 40 20 0
Hour

Fig. 3

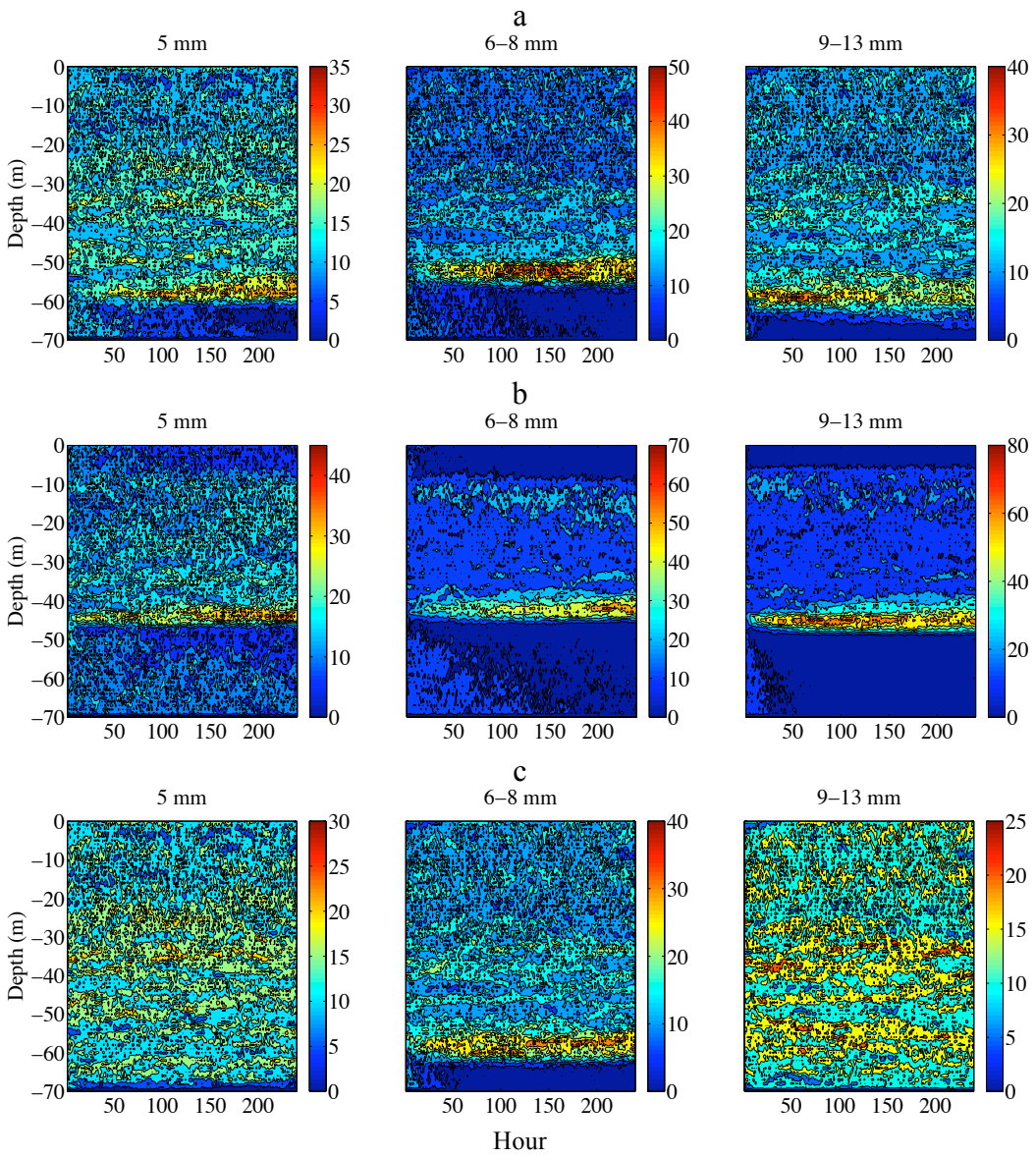

Fig. 4

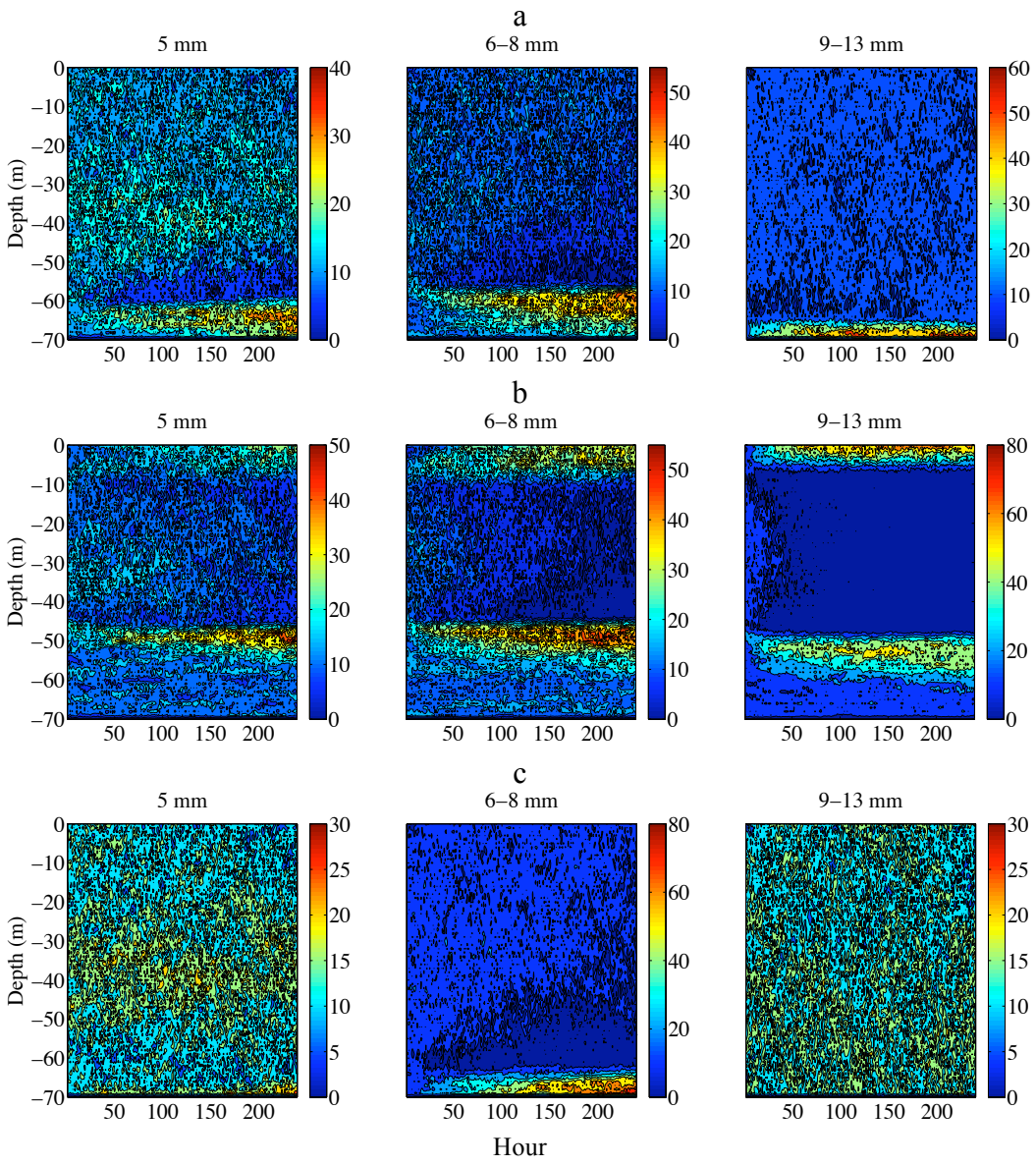

Fig. 5

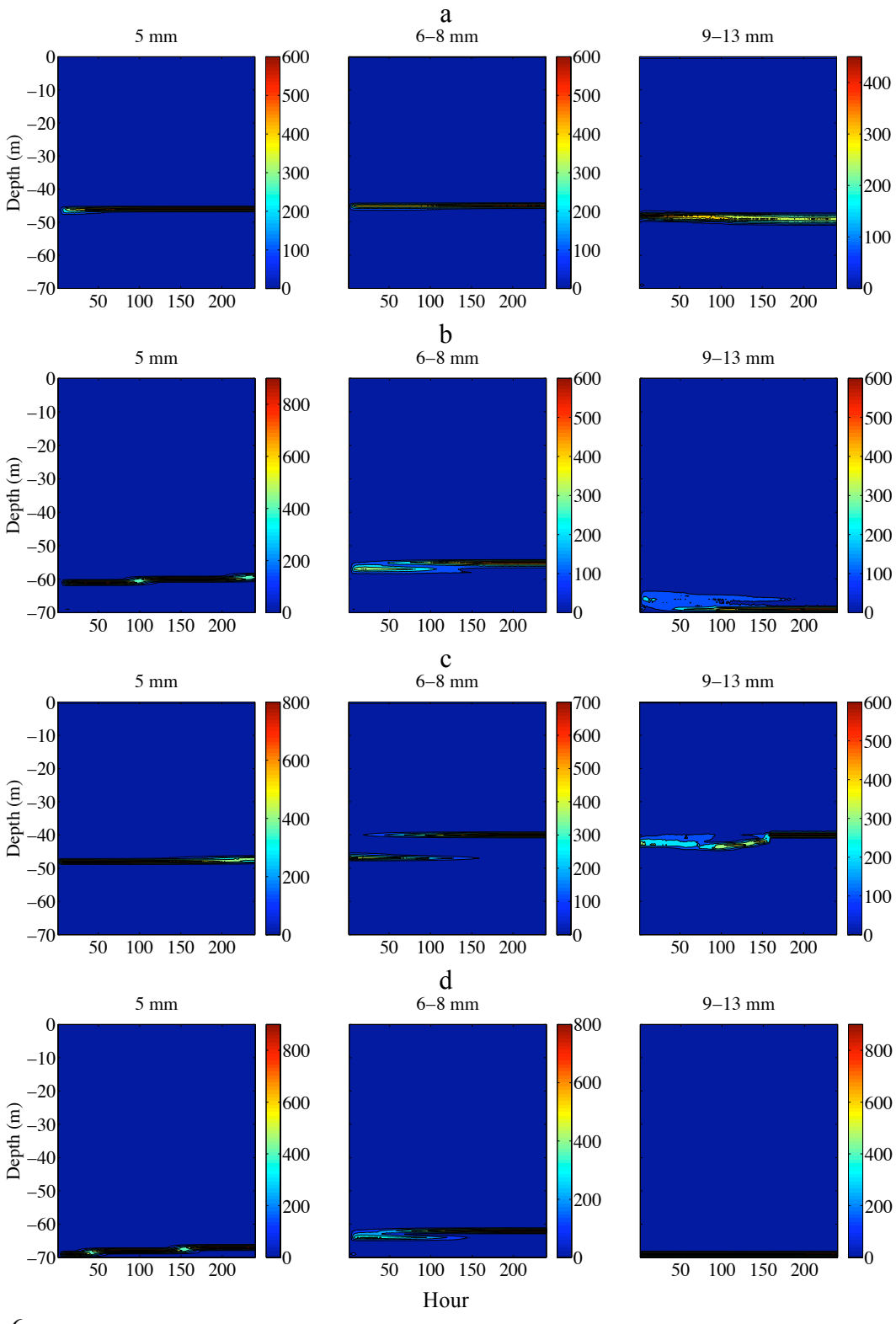
a
5 mm
6–8 mm
9–13 mm
b
5 mm
6–8 mm
9–13 mm
c
5 mm
6–8 mm
9–13 mm
d
5 mm
6–8 mm
9–13 mm
Depth (m)
Hour

Fig. 6

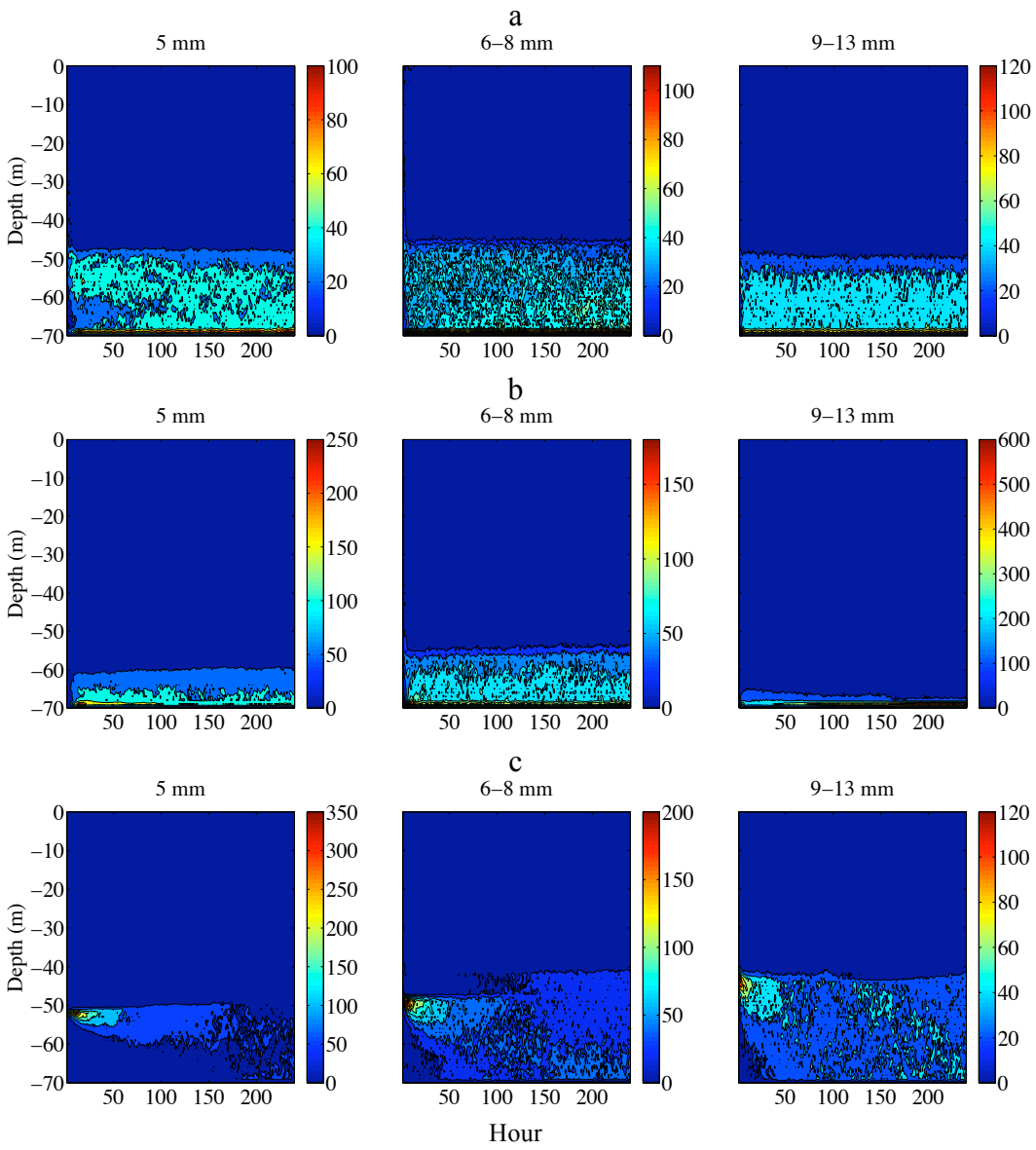

Fig. 7